Molecular Therapy
Nucleic Acids
Original Article

Role of miR-300-3p in Leydig cell function and differentiation: A therapeutic target for obesity-related testosterone deficiency

Jinlian Liang,[1,3,5] Derong Chen,[1,3,5] Ziyan Xiao,[1,3,5] Siying Wei,[1] Yuan Liu,[1] Chengzhi Wang,[2] Zhaoyang Wang,[1] Yuqing Feng,[3] Yaling Lei,[1] Meirong Hu,[1] Jingxian Deng,[3] Yuxin Wang,[1] Qihao Zhang,[1,3] Yan Yang,[1,3] and Yadong Huang[1,3,4]

[1]Department of Cell Biology, Jinan University, Guangzhou 510632, China; [2]Department of Endocrinology, Sun Yat-Sen Memorial Hospital, Sun Yat-Sen University, Guangzhou 510120, People's Republic of China; [3]Guangdong Province Key Laboratory of Bioengineering Medicine, Guangzhou 510632, China; [4]Department of Pharmacology, Jinan University, Guangzhou 510632, China

MicroRNAs (miRNAs) regulate various cellular functions, but their specific roles in the regulation of Leydig cells (LCs) have yet to be fully understood. Here, we found that the expression of miR-300-3p varied significantly during the differentiation from progenitor LCs (PLCs) to adult LCs (ALCs). High expression of miR-300-3p in PLCs inhibited testosterone production and promoted PLC proliferation by targeting the steroidogenic factor-1 (*Sf-1*) and transcription factor forkhead box O1 (*FoxO1*) genes, respectively. As PLCs differentiated into ALCs, the miR-300-3p expression level significantly decreased, which promoted testosterone biosynthesis and suppressed proliferation of ALCs by upregulating SF-1 and FoxO1 expression. The LH/METTL3/SMURF2/SMAD2 cascade pathway controlled miR-300-3p expression, in which luteinizing hormone (LH) upregulated SMAD-specific E3 ubiquitin protein ligase 2 (SMURF2) expression through methyltransferase like 3 (METTL3)-mediated *Smurf2* N6-methyladenosine modification. The *Smurf2* then suppressed miR-300 transcription by inhibiting SMAD family member 2 (SMAD2) binding to the promoter of miR-300. Notably, miR-300-3p was associated with an obesity-related testosterone deficiency in men and the inhibition of miR-300-3p effectively rescued testosterone deficiency in obese mice. These findings suggested that miR-300-3p plays a pivotal role in LC differentiation and function, and could be a promising diagnostic or therapeutic target for obesity-related testosterone deficiency.

INTRODUCTION

Adult Leydig cells (ALCs) are located in the interstitium of the mammalian testis and are the main source of testosterone production. Testosterone plays a key role in male reproduction development,[1] spermatogenesis,[2] and maintaining secondary sex characteristics. During the postnatal development, ALCs are derived from stem Leydig cells (SLCs). There are two immediate stages between ALCs and SLCs, called progenitor Leydig cells (PLCs) at postnatal day 21 and immature Leydig cells (ILCs) between postnatal days 28 and 35.[3] During puberty, proliferation of PLCs is required to increase the number of LCs. PLCs produce low amounts of testosterone, but testosterone production increases when PLCs differentiate into ALCs. LC dysfunction leads to male reproduction diseases, including testosterone deficiency, primary hypogonadism, and aspermatogenesis.[4]

Testosterone synthesis depends on the hypothalamic-pituitary-testicular axis. The hypothalamus impulsively secretes gonadotropin-releasing hormone (GnRH) to stimulate the secretion of gonadotropin-luteinizing hormone (LH) by the pituitary gland. LH binds to the LH receptor (LHCGR) on the surface of LCs to activate adenylyl cyclase (cAMP), leading to a cascade that stimulates testosterone production.[5] LH is important for LC maturation,[6] testosterone synthesis,[2] spermatogenesis,[7] and sexual organ development in men.[8] The disruption of the LH receptor gene can result in a drastic decrease in LC number and testosterone levels.[9] In addition, the transcriptional regulation of steroidogenic proteins, including steroidogenic acute regulatory (StAR),[10] cytochrome P450 family 11 subfamily A member 1 (CYP11A1),[11] 17α–hydroxylase (CYP17A1),[12] 3-beta-hydroxy-steroid dehydrogenase (HSD3β1),[13] and 17beta-hydroxy-steroid dehydrogenase (HSD17β),[11,13] also plays an important role in LC function.

MicroRNAs (miRNAs) interact with target genes by binding to the 3′ untranslated region (3′ UTR) or the coding sequence (CDS) of mRNAs and have been identified and characterized in the testis. Recent studies have demonstrated that miRNAs are important

Received 8 October 2022; accepted 21 March 2023;
https://doi.org/10.1016/j.omtn.2023.03.016.

[5]These authors contributed equally

Correspondence: Yan Yang, Department of Cell Biology, Jinan University, Guangzhou 510632, China.
E-mail: yangyan107@jnu.edu.cn
Correspondence: Yadong Huang, Department of Cell Biology, Jinan University, Guangzhou 510632, China.
E-mail: tydhuang@jnu.edu.cn

post-transcriptional regulators that play critical roles in the development and function of the testis.[14–16] Multiple miRNAs are involved in steroid hormone synthesis that takes place in LCs.[17] Indeed, miRNA expression profiling showed significant variations during PLC differentiation into ALCs, in which miR-199-5p, miR-29a-3p, miR-29b-3p, miR-29c-3p, and miR-7a-5p suppressed testosterone synthesis.[14] For example, miR-1197-3p regulates testosterone production by targeting peroxisome proliferator-activated receptor gamma coactivator 1 alpha (PPARGC1A) in goat LCs,[18] and the triclosan (TCS)-induced miR-142-5p inhibits CYP17A1 to downregulate testosterone levels.[16] These studies demonstrate that miRNAs play an important role in androgen synthesis and development in LCs; however, the functions and mechanisms of miRNAs in LC regulation remain largely unknown.

In this study, we found that the expression level of miR-300-3p significantly varied at different developmental stages in LCs, with high expression in PLCs and low expression in ALCs. Previous studies showed that miR-300-3p plays a regulatory role in cell proliferation,[19,20] differentiation,[21] tumorigenesis, and metastasis.[22,23] However, the role of miR-300-3p in LC differentiation and testosterone synthesis has not been reported. Our results suggest that miR-300-3p overexpression inhibits testosterone synthesis and promotes PLC proliferation *in vitro* and *in vivo*. MEETL3-mediated m^6A modification is critical for miR-300-3p expression, which is associated with obesity-related testosterone deficiency. Inhibition of miR-300-3p in testis of high-fat diet (HFD) mice rescued obesity-related testosterone deficiency, revealing that miR-300-3p is a potential therapeutic target for obesity-related testosterone deficiency.

RESULTS

miR-300-3p suppresses testosterone synthesis in LCs by targeting *Sf-1*

We first assessed miR-300-3p expression in the testes using *in situ* hybridization. miR-300-3p expression was observed in both young (3-week-old) and adult (8-week-old) male mice, but was highly expressed in the testis interstitium of young mice (Figure 1A, Figure S1A). We isolated PLCs from young mouse testes and ALCs from adult mouse testes (Figure S1B) and used quantitative reverse transcription polymerase chain reaction (qRT-PCR) to detect the expression of miR-300-3p in these cell types. The level of miR-300-3p was significantly decreased in ALCs (Figure 1B). To determine whether the loss of miR-300-3p expression was accompanied by alterations in steroidogenic proteins, we examined the expression of steroidogenic factor-1 (SF-1), CYP11A1, and StAR in PLCs and ALCs. The results showed that SF-1, CYP11A1, and StAR levels were significantly higher in ALCs than in PLCs (Figures 1C and S1C). Moreover, the reduction in miR-300-3p was correlated with an increase in steroidogenic proteins and testosterone levels (Figure 1D), consistent with an inverse correlation between miR-300-3p expression and testosterone production in LCs. Therefore, we hypothesized that miR-300-3p plays a role in testosterone biosynthesis.

To investigate the function of miR-300-3p, ALCs were transfected with an miR-300-3p mimic to increase exogenous miR-300-3p, while PLCs were transfected with an miR-300-3p inhibitor to block miR-300-3p. The miR-300-3p mimic significantly suppressed testosterone production in ALCs (Figure 1E). In contrast, testosterone levels in PLCs increased in response to the miR-300-3p inhibitor (Figure 1F). Collectively, these results showed that miR-300-3p is involved in testosterone synthesis in LCs.

We also examined the expression of SF-1, CYP11A1, and StAR after LCs transfected with either the miR-300-3p mimic or inhibitor. The results showed that the miR-300-3p mimic downregulated the expression of SF-1, CYP11A1, and StAR (Figures 1G and S1B), while in contrast, the levels of SF-1, CYP11A1, and StAR were significantly upregulated in PLCs transfected with the miR-300-3p inhibitor (Figures 1H and S1C). To further reveal the molecular mechanism of miR-300-3p involvement in testosterone synthesis, TargetScan was used to predict the targets of miR-300-3p. Among the steroidogenic genes, *Sf-1* was identified as a target of miR-300-3p (Figure 1I). *Sf-1* is a key transcription factor of steroidogenic genes, and regulates steroidogenic gene expression and testosterone production in LCs.[24–27] To confirm if miR-300-3p can directly bind to the 3′-UTR of *Sf-1*, luciferase reporter vectors containing the wild-type (WT) or mutated 3′-UTR of *Sf-1* were co-transfected with miR-300-3p mimic or negative control (NC) mimic into HEK293T cells. The miR-300-3p mimic significantly suppressed the luciferase activity of the WT reporter vector, whereas the miR-300-3p binding site mutants did not (Figure 1J). Exogenous overexpression of miR-300-3p specifically downregulated *Sf-1* expression and this effect could be rescued by *Sf-1* overexpression (Figure 1K). Similar to the effects of the miR-300-3p mimic, blocking the expression of *SF-1* significantly downregulated the expression of steroidogenic proteins (CYP11A1 and StAR) (Figure 1L) and testosterone production (Figure 1M).

Western blotting also demonstrated that the miR-145-5p mimics downregulated CYP11A1 and StAR protein expression (Figures 2F–2H). To further support a role for miR-145-5p, we used miR-145-5p inhibitor to selectively block the activity of miR-145-5p in ILCs. Conversely, ILCs transfected with miR-143-3p inhibitor exhibited significant increases in levels of testosterone, compared with control cells. And the expression of steroidogenic genes and protein were significantly downregulated by miR-145-5p inhibitor.

Results demonstrate that miR-145-5p regulates steroidogenic gene expression and testosterone biosynthesis. In addition, the level of free cholesterol that constitutes the pool used for steroidogenesis in LCs was analyzed, and Oil Red O staining showed that miR-145-5p overexpression resulted in lipid accumulation (Figure 2I). Moreover, transmission electron microscopy also revealed the formation of lipid droplet clusters in LCs overexpressing miR-145-5p (Figure 2J). In contrast, no obvious aggregation of lipid droplets was observed in cells treated with mimic-NC. These results suggest that miR-145-5p overexpression causes defects in cholesterol metabolism in Leydig cells, subsequently inhibiting testosterone production.

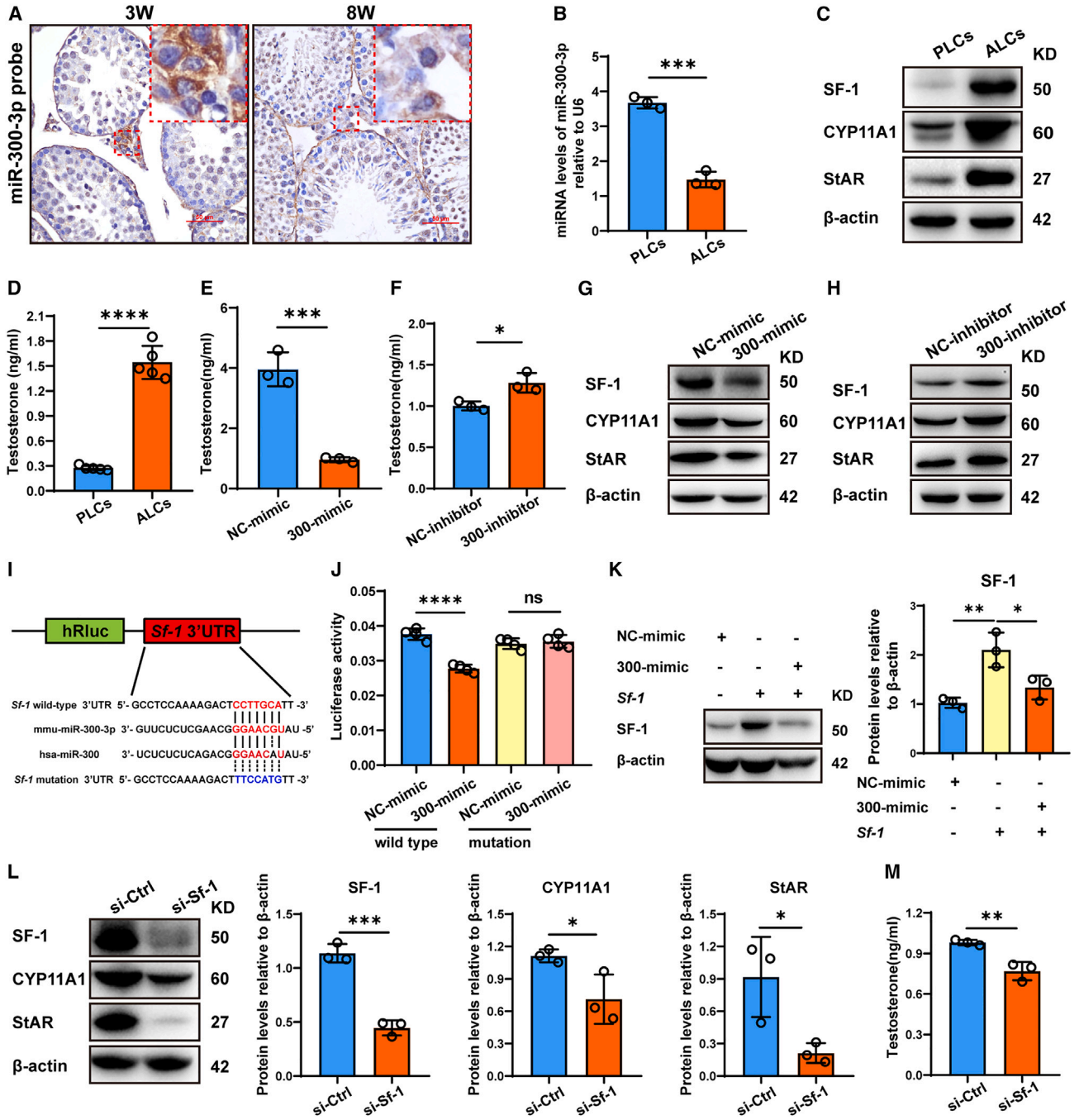

Figure 1. miR-300-3p directly targets *Sf-1* to suppress testosterone production

(A) *In situ* hybridization images illustrating that miR-300-3p is mainly localized in interstitial spaces in the testis (red arrow). Scale bar, 50 μm. (B) RT-qPCR results showing miR-300-3p expression in PLCs and ALCs. PLCs and ALCs were isolated from 3- and 8-week-old mouse testes, respectively. (C) Expression levels of steroidogenic proteins SF-1, CYP11A1, and StAR in PLCs and ALCs. (D) Radioimmunoassay assay (RIA) analysis of testosterone concentrations in PLC and ALC cell culture supernatants. (E and F) Testosterone concentrations in culture supernatant from LCs transfected with an miR-300-3p mimic or inhibitor. (G) and (H) Protein levels of SF-1, CYP11A1, and StAR in LCs transfected with an miR-300-3p mimic or inhibitor. (I) TargetScan predicted that miR-300-3p binds to the 3′-UTR of *SF-1*. (J) HEK293T cells were co-transfected with luciferase reporter vectors (psi-check 2 containing the wild-type or 3′-UTR *SF-1* mutants) and an miR-300-3p or NC mimic. The relative Renilla luciferase activity was measured and normalized to firefly luciferase activity. (K) Protein level of SF-1 in LCs co-transfected for 48 h with *Sf-1* overexpression vector and an miR-300-3p or NC mimic. (L) Protein levels of SF-1, CYP11A1, and StAR in LCs transfected with *Sf-1* siRNA. (M) Testosterone concentrations in culture supernatants from LCs transfected with *Sf-1* siRNA. All data are presented as the mean ± SD from at least three independent experiments. *p < 0.5, **p < 0.01, ***p < 0.001, ****p < 0.0001, ns = not significant.

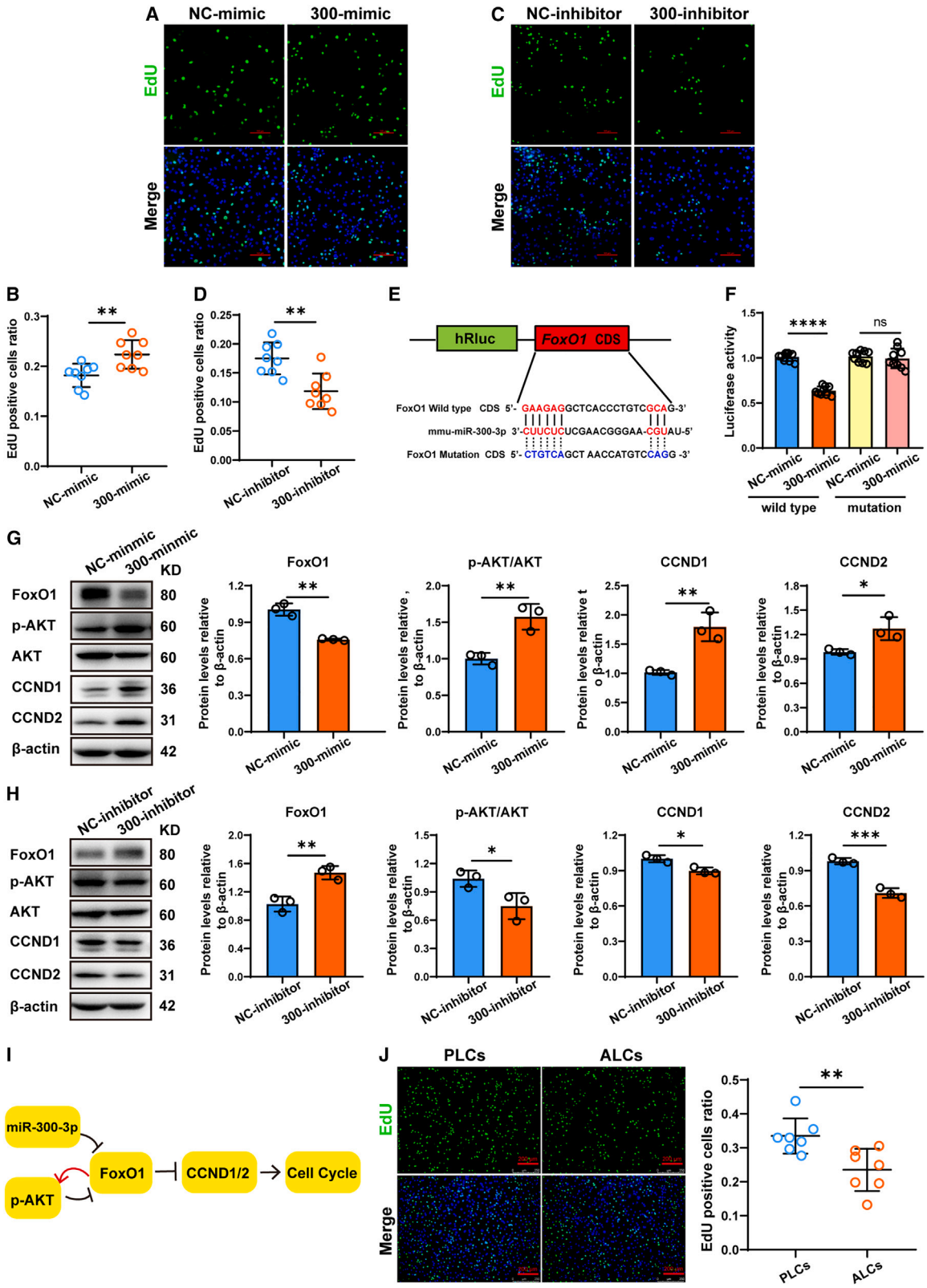

(legend on next page)

These results suggested that miR-300-3p expression decreased as LCs differentiated from PLCs into ALCs, and the reduction of miR-300-3p upregulated the expression of CYP11A1 and StAR by targeting the 3′-UTR of *Sf-1*, which subsequently promoted testosterone biosynthesis in ALCs.

miR-300-3p regulates LC proliferation by targeting *FoxO1*

To investigate whether miR-300-3p overexpression suppresses testosterone production by inhibiting PLC proliferation, an EdU incorporation assay was used to estimate LC proliferation after miR-300-3p mimic or inhibitor treatment. The miR-300-3p mimic increased the number of EdU-positive cells (Figures 2A and 2B) while the miR-300-3p inhibitor decreased the number of EdU-positive cells (Figures 2C and 2D). These results suggested that miR-300-3p overexpression had a suppressive effect on testosterone production that not due to cell proliferation inhibition. We further revealed the mechanism by which miR-300-3p promotes PLC proliferation and found that *Forkhead box transcription factor O1* (*FoxO1)* is a putative target of miR-300-3p (Figure 2E). The miR-300-3p mimic significantly suppressed the luciferase activity of the WT reporter vector, whereas mutation of the potential miR-300-3p binding site did not (Figure 2F). FoxO1 is a growth-attenuating winged helix transcription factor protein that serves as a substrate for phosphoinositide protein kinase B (AKT) and mediates the feedback activation of AKT.[28] We assessed AKT and FoxO1 signaling by measuring the protein levels of AKT, phosphorylated AKT (p-AKT), FoxO1, cell cycle-associated proteins cyclin D1 (CCND1), and cyclin D2 (CCND2). We found that miR-300-3p overexpression inhibited FoxO1 expression and increased p-AKT, CCND1, and CCND2 expression (Figure 2G). The opposite effect was observed in cells transfected with miR-300-3p inhibitor (Figure 2H). These results suggested that miR-300-3p overexpression downregulated the expression of *FoxO1*, which increased p-AKT via a feedback loop that promotes the proliferation of LCs (Figure 2I). When we examined the proliferation of PLCs and ALCs, we observed more EdU-positive cells in PLCs than in ALCs (Figure 2J), which indicated that PLCs have a stronger proliferation ability than ALCs. The change in proliferation ability in PLCs and ALCs was consistent with the miR-300-3p regulation pattern. The loss of miR-300-3p induced the differentiation of PLCs into ALCs and promoted testosterone biosynthesis.

The functions of miR-300-3p *in vivo*

To further investigate whether miR-300-3p suppresses testosterone production *in vivo*, miR-300-3p agomir and antagomir were injected into the interstitium of adult mouse testes (Figure 3A), while control mice were injected with PBS and the mock control mice were injected with corresponding scrambled miRNAs. Two weeks after the treatment, hematoxylin-eosin (H&E) staining of teste tissue samples showed no obvious changes (Figures S2A and S2B); neither the miR-300-3p agomir nor antagomir resulted in a significant number of apoptotic cells (Figures S2C and S2D). These results suggested that the miR-300-3p agomir and antagomir did not exhibit cytotoxicity in the testes. We then confirmed the efficacy of miR-300-3p agomir and antagomir injections using *in situ* hybridization. The miR-300-3p agomir significantly elevated the expression of miR-300-3p in the interstitium of the testes, while the miR-300-3p antagomir successfully decreased the amount of miR-300-3p present in these tissues (Figures 3B, 3C, S2E, and S2F).

Serum was collected to determine testosterone concentrations 14 days after the miR-300-3p agomir or antagomir injection. The results showed that the miR-300-3p agomir significantly downregulated the level of serum testosterone, while the miR-300 antagomir dramatically increased serum testosterone production when compared with that of the controls (Figures 3D and 3E). Free cholesterol is a pool used for steroidogenesis in LCs and Oil Red O staining was used to analyze the level of free cholesterol. We found that a large number of lipid droplets accumulated in the interstitium of testes after miR-300-3p agomir treatment (Figure 3F) while miR-300 antagomir treatment decreased lipid droplet accumulation compared with normal control (Figure 3G). Immunofluorescence analysis revealed that the expression of CYP17A1 was upregulated by miR-300-3p agomir, which showed a consistent change in serum testosterone production (Figures 3H, 3I, and S2G). In addition, the miR-300-3p agomir significantly decreased the levels of SF-1, CYP11A1, StAR, and FoxO1; upregulated the expression of CCND1 and CCND2 in testis (Figures 3J and S2G). In contrast, the miR-300 antagomir significantly increased the protein levels of SF-1, CYP11A1, StAR, and FoxO1; and significantly decreased the protein levels of CCND1 and CCND2 (Figures 3K and S2H). Taken together, these results confirmed that miR-300-3p modulated testosterone synthesis and LC proliferation by targeting SF-1 and FoxO1, respectively. Overexpression of miR-300-3p in adult male testes may induce dysfunction of testosterone secretion in LCs.

miR-300-3p is a therapeutic target for obesity-related testosterone deficiency

We examined whether abnormally high miR-300-3p expression results in obesity-related testosterone deficiency. RIA was used to measure the serum testosterone levels of lean and obese men. The result showed that mean testosterone concentrations in lean men were 8.12 ng/mL, and obese men had subnormal levels of 6.00 ng/mL

Figure 2. miR-300-3p targets *FoxO1* to promote LC proliferation

(A–D) EdU assays show the effect of the miR-300-3p mimic and inhibitor on LC proliferation. NC-mimic = mimic negative control, NC-inhibitor = inhibitor negative control. Scale bar, 100 μm. (E) miR-300-3p was predicted to bind to the CDS region of *FoxO1* mRNA. (F) HEK293T cells co-transfected with luciferase reporter vectors (psi-check 2 containing the wild-type or mutated *FoxO1* CDS region) and miR-300-3p mimic or NC mimic. The relative Renilla luciferase activity was normalized to the firefly luciferase activity. (G and H) Protein levels of FoxO1, p-AKT, AKT, CCND1, and CCND2 in LCs transfected with miR-300-3p mimic, miR-300-3p inhibitor, or the respective NC. (I) Schematic diagram of the miR-300-3p activating AKT pathway. (J) Cell proliferation was assessed by EdU incorporation in PLCs and ALCs. Scale bar, 200 μm. Data are presented as the mean ± SD from at least three independent experiments. *$p < 0.5$, **$p < 0.01$, ***$p < 0.001$, ****$p < 0.0001$, ns = not significant.

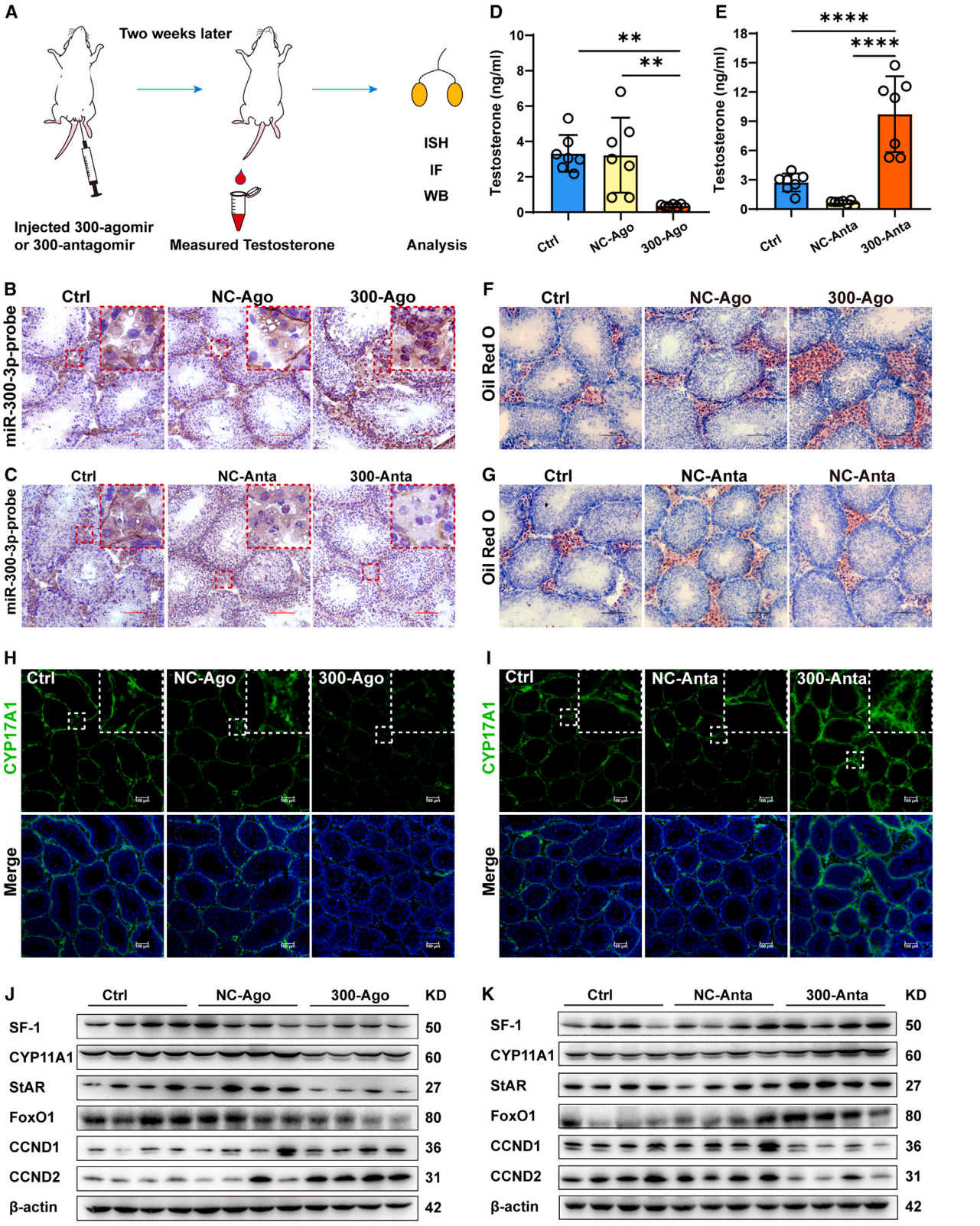

(legend on next page)

(Figure 4A). Circulating miR-300-3p in serum samples was detected by qRT-PCR, which showed that miR-300-3p was significantly increased in obese men compared with that in lean men (Figure 4B), suggesting that high miR-300-3p expression was associated with low testosterone levels (Figure 4C). These results demonstrated that abnormally high expression of miR-300-3p may be an important regulator of obesity-related testosterone deficiency.

We further explored the role of miR-300-3p in obesity-related testosterone deficiency in male mice fed an HFD, 60% kcal fat) or normal chow (Figure 4D). After 12 weeks, the weight of HFD-fed mice (40.7 g) significantly increased by more than 40% compared with that of chow-fed mice (28.3 g) (Figure 4E). Serum testosterone concentrations in HFD mice was also dramatically reduced (Figure 4F) and miR-300-3p expression in serum was significantly elevated (Figure 4G) compared with that in chow-fed mice. In addition, qRT-PCR and *in situ* hybridization showed that the expression of miR-300-3p in the testes of HFD mice was significantly higher than that in the testes of chow-fed mice (Figures 4H and 4I). These data suggested that increased miR-300-3p expression in the testes of adult males may be involved in the modulation of obesity-related testosterone deficiency.

We further examined the effects of miR-300-3p on testosterone synthesis using an obese mouse model. HFD mice were treated with an miR-300-3p or NC inhibitors once a week for 4 weeks. Untreated mice fed normal chow were used as normal controls. The miR-300-3p inhibitor effectively downregulated the expression of miR-300-3p in HFD mice to levels that were comparable to that of the normal control (Figure 4J). Serum was collected for testosterone measurement after treatment with the miR-300-3p inhibitor, which showed that testosterone levels in HFD mice were similar to the normal levels (Figure 4K). The protein levels of SF-1 and FoxO1 in the testes were significantly downregulated in the HFD-fed mice; however, the miR-300-3p inhibitor rescued SF-1 and FoxO1 expression levels (Figure 4L). These results indicated that miR-300-3p silencing can rescue testosterone production in HFD mice and therefore, miR-300-3p is a potential therapeutic target in testosterone deficiency.

N6-adenosine methylation regulates the expression of miR-300-3p in LCs via the SMURF2/p-SMAD2 axis

The N6-adenosine methylation (m^6A) modification is important for regulating the stability of m^6A modified RNAs.[29,30] It has also been reported that m^6A is involved in the regulation of hepatic lipid and glucose metabolism in HFD mice[31]; therefore, we examined whether m^6A modification was involved in regulating miR-300-3p expression. Lower m^6A levels were observed in HFD mouse testes than in chow-fed mice (Figure 5A). To further explore the enzymes that mediate m^6A methylation in HFD, we examined the expression of methylation transferases (METTL3 and METTL14) and demethylase (ALKBH5) with western blotting. The level of METTL3 in the testes of HFD mice was significantly lower than that in the normal control mice, while the expression of METTL14 and ALKBH5 did not significantly change between HFD and chow-fed mice (Figures 5B and S3A). Thus, we hypothesized that miR-300-3p expression was modulated by METTL3. *Mettl3* knockdown and overexpression in LCs were used to determine the role of METTL3 in the regulation of miR-300-3p expression. We found that *Mettl3* overexpression significantly downregulated the expression of miR-300-3p (Figures 5C and 5D), while in contrast, *Mettl3* siRNA increased miR-300-3p expression (Figures 5E and 5F). Moreover, we found that *Mettl3* overexpression downregulated the expression of miR-300-3p, which was accompanied by decreased levels of phosphorylated SMAD2 (p-SMAD2) and increased levels of SMAD-specific E3 ubiquitin protein ligase 2 (SMURF2) (Figures 5G and S3B). However, the knockdown of METTL3 led to the opposite results (Figures 5H and S3C). These data suggested that METTL3 controls the expression of miR-300-3p via SMURF2 and SMAD2.

To elucidate the regulatory relationship among METTL3, SMURF2, p-SMAD2, and miR-300-3p, we focused on the GGACU-binding motif of *Mettl3*, a subunit of m^6A methyltransferase. The METTL3 binding motif "GGAC" was found in the 3′-UTR of *Smurf2* (Figure 5I). *Mettl3* overexpression significantly increased *Smurf2* mRNA levels, while *Mettl3* knockdown resulted in a reduction in *Smurf2* expression. To confirm whether the *Smurf2* transcript was regulated by *Mettl3*, we generated luciferase reporter vectors containing firefly and Renilla luciferases, followed by the 3′-UTR of *Smurf2* WT or mutation sequences of each m^6A site (i.e., "GGAC" to "GGGC") (Figure 5J). The 3′-UTR luciferase reporter vectors of *Smurf2* and pcDNA3.1-*Mettl3* were co-transfected into HEK293T cells. *Mettl3* overexpression significantly increased the luciferase activity of the WT vector (Figure 5K), while the mutation of sites 1 (MU1, NM_001362894.1:2853–2856) and 2 (MU2, NM_001362894.1:2929–2932) effectively attenuated this increase. Simultaneous mutations at all five sites (MU6) also downregulated the luciferase activity, which showed an overlay of multiple effects. These results suggested that *Smurf2* mRNA is modified by m^6A methylation.

Smurf2 is a negative regulator of the transforming growth factor (TGF)-β signaling pathway, which degrades phosphorylated SMAD2. Our results suggested *Mettl3* overexpression increased the

Figure 3. The functions of miR-300-3p in vivo

(A) Schematic of miR-300-3p agomir and antagomir injection into interstitium of adult mouse testes. (B and C) miR-300-3p expression in testes was detected by *in situ* hybridization 2 weeks after miR-300-3p agomir and antagomir treatment. Scale bar, 100 μm. (D and E) Serum testosterone was measured by radioimmunoassay after miR-300-3p agomir and antagomir treatment. (F and G) Representative images of Oil Red O staining 2 weeks after miR-300-3p agomir and antagomir injections. Scale bar, 100 μm. (H and I) Detection of CYP17A1 (green) in testes by immunofluorescence 2 weeks after miR-300-3p agomir and antagomir injection. Scale bar, 100 μm. (J and K) SF-1, CYP11A1, StAR, FoxO1, CCND1, and CCND2 protein expression in testes was analyzed by western blotting 2 weeks after miR-300-3p agomir and antagomir injections. All data are shown as the mean ± SD from at least six animals. *p < 0.5, **p < 0.01, ***p < 0.001, ****p < 0.0001.

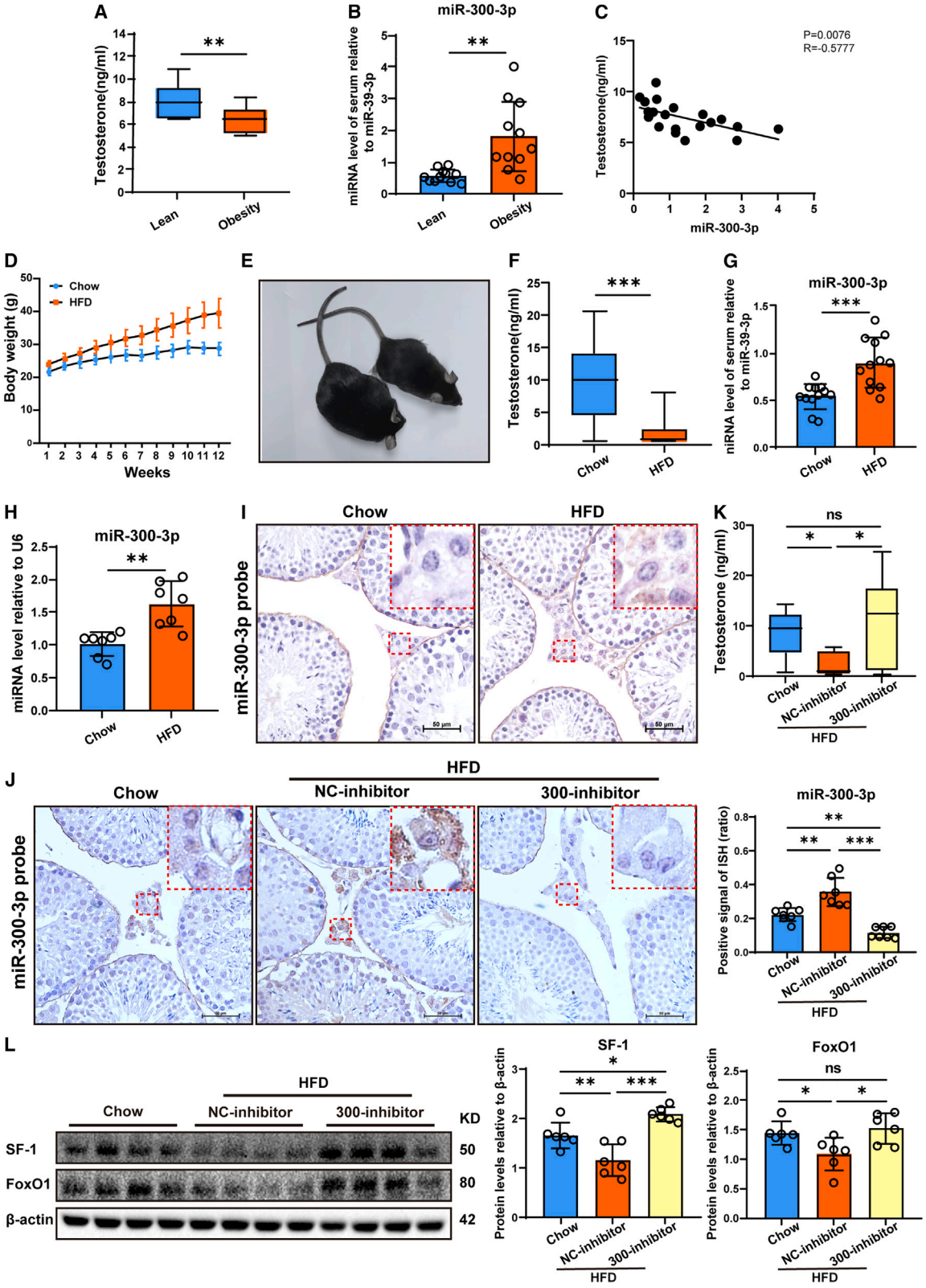

(legend on next page)

mRNA level of *Smurf2*, and inhibition of *Mettl3* downregulated *Smurf2* expression (Figures 5L and 5M). Moreover, the increased level of SMURF2 was associated with a decrease in p-SMAD2, while the expression of p-SMAD2 was increased by the inhibition of SMURF2. These results suggested that decreased METTL3 suppressed p-SMAD2 expression by upregulating the level of SMURF2. Moreover, we found *Smad2* is a potential transcription factor that may bind to the promoter of the miR-300 gene (Figure 5N). The expression of miR-300-3p was significantly elevated by *Smad2* overexpression (Figure 5O). To determine whether *Smad2* can bind to the miR-300 promoter, we generated luciferase reporter constructs driven by the miR-300 promoter or the promoter with a mutated *Smad2* binding site (Figure 5P). Luciferase activity was strongly increased by *Smad2* (Figure 5Q); however, when the binding site was mutated, the fluorescence activity significantly decreased (Figure 5Q), confirming that *Smad2* could bind to the promoter of miR-300 and subsequently initiate miR-300 transcription. These results confirmed that METTL3 regulates the expression of miR-300-3p via the SMURF2/SMAD2 axis (Figure 5R).

METTL3 is regulated by LH

LH is an important hormone that promotes the synthesis of LC and testosterone.[9,32] We examined the levels of serum LH and testosterone in male mice at different developmental stages. LH and testosterone levels progressively increased from 3 to 5 weeks after birth (Figures 6A and 6B). Moreover, RNA m^6A levels and METTL3 expression also increased significantly during testis development between 3 and 5 weeks (Figures 6C, 6D, S4A, and S4B), while the expression of miR-300-3p decreased (Figure S4C). To investigate whether LH affects m^6A modification levels in LCs, we measured the expression of METTL3 in LCs stimulated with LH at different concentrations (0, 5, 10, and 50 ng/mL) and found that the levels of METTL3 increased as LH concentrations increased. Upregulation of METTL3 expression also contributed to the increase in SMURF2, which then downregulated p-SMAD2 expression (Figures 6E and 6F) and eventually led to a reduction in miR-300-3p (Figure 6G). These data demonstrated that METTL3 was regulated by LH, which can drive changes in miR-300-3p expression in LCs.

In summary, the LH/METTL3/SMURF2/SMAD2/miR-300-3p pathway tightly controls LC proliferation, differentiation, and testosterone synthesis by targeting FoxO1 and SF-1. In ALCs, LH induced METTL3 and SMURF2 expression by promoting METTL3 mediated m^6A modification of *Smurf2*, which suppressed miR-300-3p transcription by inhibiting p-SMAD2 levels. The reduction of miR-300-3p improved testosterone production and inhibited proliferation in ALCs by upregulating SF-1 and FoxO1. The abnormally high expression of miR-300-3p observed in ALCs was involved in the regulation of obesity-related testosterone deficiency (Figure 7).

DISCUSSION

LC differentiation and function depend on fine-tuning gene expression regulation.[33,34] LCs in mammals progressively improve their capacity to synthesize testosterone during development and their differentiation from PLCs to ALCs, peaking in ALCs.[35,36] Therefore, we hypothesized that some genes dynamically regulate LC function during LC differentiation. In this study, we observed that high miR-300-3p expression in PLCs progressively decreased with differentiation, suggesting that miR-300-3p is involved in regulating LC differentiation and function. However, the function of miR-300-3p in LCs has not yet been elucidated.

In this study, we found that overexpression of miR-300-3p in ALCs inhibited the expression of SF-1 and testosterone production by binding to the 3′-UTR of the *Sf-1* gene, whereas inhibition of miR-300-3p upregulated SF-1 expression and promoted testosterone synthesis. SF-1 is an indispensable transcriptional regulator of LC development and survival that regulates the expression of steroidogenic genes[24–26,37] by binding to their promoters to enhance gene transcription. Ectopic overexpression of *Sf-1* directly converted non-steroidal producing cells (e.g., mesenchymal cells, embryonic stem cells, and fibroblasts) into functional Leydig-like cells,[38–41] illustrating the importance of SF-1 in testosterone synthesis and LC differentiation. In this study, we observed a gradual increase in SF-1 expression in LCs during their differentiation from PLCs to ALCs, suggesting that SF-1 is dynamically modulated by miR-300-3p during LC differentiation. We asked whether the abnormal increase in miR-300-3p expression in adulthood caused LC dysfunction and observed that low levels of serum testosterone were accompanied by a significant increase in miR-300-3p levels in both obese men and HFD mice. It has been reported that obese men have subnormal serum testosterone concentrations[42–44]; however, the relationship between serum testosterone levels and obesity remains complex and the mechanism underlying obesity-induced testosterone deficiency has not been elucidated. We found that above-normal levels of miR-300-3p in obese men were correlated with testosterone deficiency, further confirming the role of miR-300-3p in obesity-related testosterone deficiency. The results from HFD mice treated with an miR-300-3p inhibitor suggested that miR-300-3p inhibition could effectively rescue low serum testosterone levels caused by obesity. These results highlight a vital role of miR-300-3p in regulating testosterone synthesis and could be a therapeutic target for testosterone deficiency.

Figure 4. miR-300-3p inhibitor rescue testosterone deficiency

(A) Serum testosterone concentrations in obese and lean adult men. (B) The expression level of serum miR-300-3p in obese and lean men was determined by qRT-PCR. (C) Analysis of the association between miR-300-3p expression and testosterone production in the serum. (D and E) Body weight change in chow-fed and HFD mice. (F) Serum testosterone levels in chow-fed and HFD mice. (G) Serum miR-300-3p expression in chow-fed and HFD mice. (H) Level of miR-300-3p expression in the testes of chow-fed and HFD mice. (I) Detection of miR-300-3p (red arrows) in testes of chow-fed and HFD mice by *in situ* hybridization. Scale bar, 50 μm. (J) miR-300-3p expression (red arrow) in testes after miR-300-3p inhibitor or NC inhibitor treatment. Scale bar, 50 μm. (K) Serum testosterone levels in HFD mice treated with miR-300-3p or NC inhibitors for 4 weeks. (L) The expression of SF-1 and FoxO1 in mouse testes after treatment with miR-300-3p or NC inhibitors. All data are shown as the mean ± SD, $^*p < 0.05$, $^{**}p < 0.01$, $^{***}p < 0.001$, $^{****}p < 0.0001$, and ns = not significant.

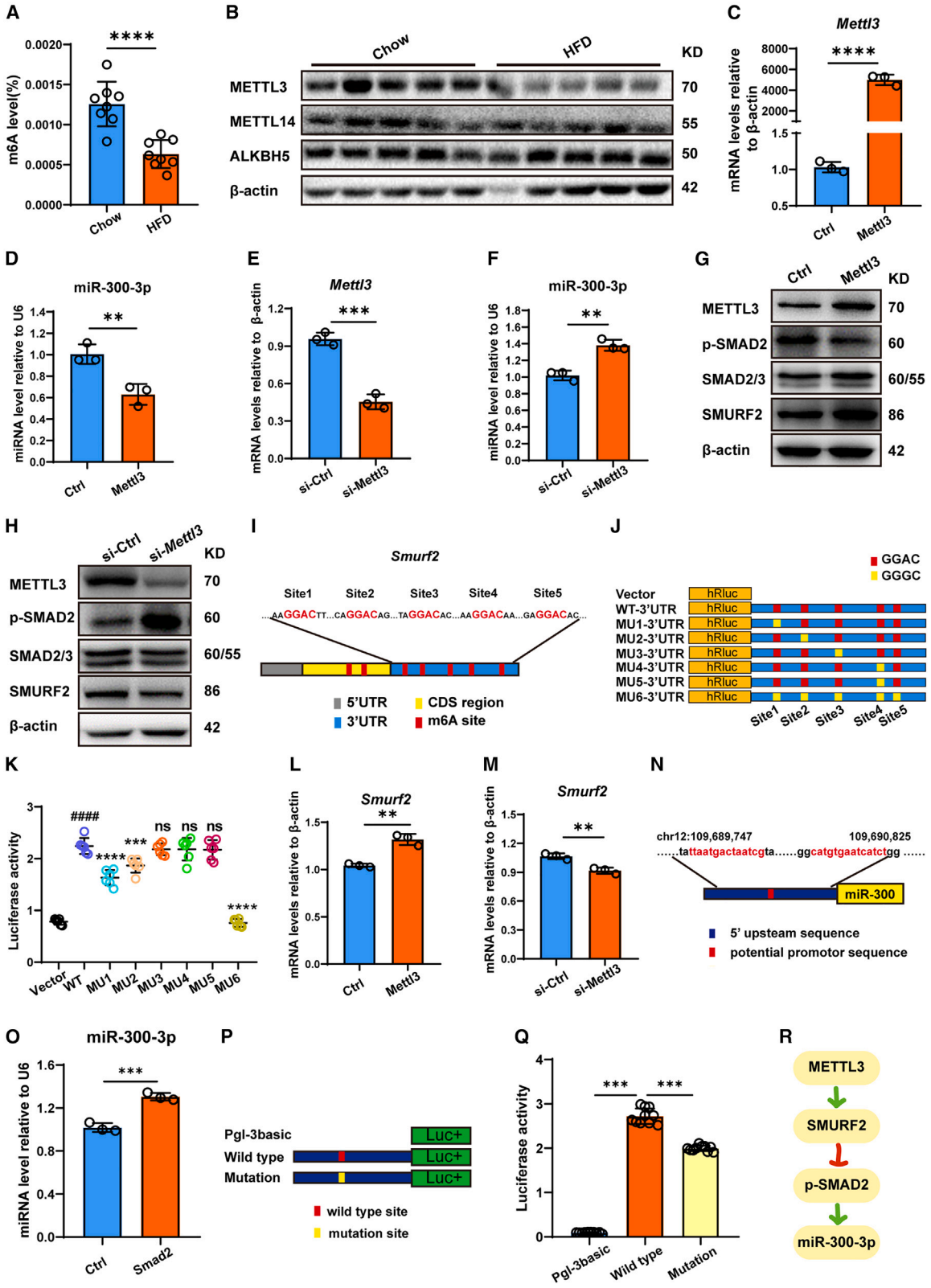

(legend on next page)

In addition, miR-300-3p modulated LC proliferation by targeting the CDS region of the *FoxO1* gene. In PLCs, high miR-300-3p expression downregulated *FoxO1* expression by binding to its CDS regions, which facilitated PLCs proliferation. However, low miR-300-3p expression upregulated *FoxO1* expression in ALCs and blocked their proliferation. Previous research suggested that miRNAs combine the targeting of CDS and 3′-UTR regions to flexibly tune the timescale and magnitude of their post-transcriptional regulatory effects.[45] These miRNAs inhibit translation by binding to sites located in the CDS of genes and trigger mRNA degradation by binding to the sites located in the 3′-UTR of genes.[46] While large numbers of miRNAs can regulate genes post-transcriptionally by binding to the target 3′-UTR regions, there are only a few reports of those that bind to CDS regions to modulate gene expression.[47] In this study, we found *FoxO1* expression could be modulated through the binding of miR-300-3p to the CDS regions, which provides new evidence for this relatively uncommon mechanism. Moreover, the FoxO1 subfamily has emerged as a shared component among pathways that regulate diverse cellular functions, such as differentiation, metabolism, proliferation, and survival.[48] It has been reported that TGF-β1-modulated cardiac fibroblast differentiation is prevented by the downregulation of FoxO1 and enhanced by FoxO1 overexpression.[49] In addition, centrosomal protein 55 overexpression causes male-specific sterility in mice by suppressing FoxO1 nuclear retention through the sustained activation of PI3K/Akt signaling.[50] In our study, FoxO1-mediated feedback promoted AKT activation, to facilitate PLC proliferation. As a result of the differentiation of PLCs into ALCs, their proliferation was suppressed. Taken together, our study demonstrated that miR-300-3p directly targets and negatively regulates the expression of SF-1 and FoxO1 to modulate the differentiation and function of LCs.

We also investigated the molecular mechanisms underlying the expression of miR-300-3p. We found that METTL3 mediated m^{6}A modification of *Smurf2* mRNA as an important regulator of miR-300-3p expression. It has been shown that METTL3 is sufficient to promote miRNA maturation, and m^{6}A modification is a key post-transcriptional modification that induces the initiation of miRNA biogenesis.[51] Accumulating evidence has confirmed that reduced expression or loss-of-function mutations in METTL14 may result in a decrease in m^{6}A levels. It has been reported that m^{6}A is involved in regulating lipid metabolism in HFD mice.[31,52,53] Moreover, m^{6}A modification modulates testosterone synthesis in LCs.[54] In this study, a progressive increase in *METTL3* expression was detected in LCs during their differentiation from PLCs to ALCs. The m^{6}A mRNA modification level and METTL3 expression were significantly decreased in the testes of HFD mice compared with that in chow-fed mice. Overexpression of *Mettl3* suppressed miR-300-3p expression in LCs, while its inhibition upregulated miR-300-3p expression, which demonstrated that METTL3 regulates the transcription of miR-300-3p. It was reported that m^{6}A regulates gene transcription or protein expression by regulating the methylation levels at a specific motif, such as "RRAC."[55] However, the "RRAC" motif was not found in the miR-300 mRNA, indicating that m^{6}A may regulate miR-300-3p expression through other molecules. We identified the m^{6}A methylation modification sites of *Smurf2*, a ubiquitin E3 ligase of SMADs that negatively regulates TGF-β signaling by promoting ubiquitin degradation of phosphorylated SMAD2.[56] SMAD2 binds to the promoter of miR-300, thereby increasing miR-300 expression, while METTL3 downregulated *p*-SMAD2 by increasing *Smurf2* transcription, thus inhibiting the transcription of miR-300-3p. Finally, we demonstrated that METTL3 expression is regulated by LH. When LCs were stimulated with LH at different concentrations, the levels of METTL3 increased in response to increasing concentrations of LH and miR-300-3p decreased significantly. This trend is consistent with the expression pattern that increased MEETL3 is accompanied by a gradual increase in serum LH and testosterone levels during LC differentiation from PLCs to ALCs. However, the mechanism through which LH regulates METTL3 expression remains unclear. It would be interesting to explore this issue in future research.

Together, our results highlight the vital role of the LH/METTL3/SMURF2/SMAD2/miR-300-3p axis in regulating LC differentiation and testosterone synthesis through the targeting of FoxO1 and SF-1 expression. The aberrant expression of miR-300-3p induces LC dysfunction and, thus, may serve as a diagnostic marker or therapeutic target for obesity-related testosterone deficiency.

MATERIALS AND METHODS

Animals

Kunming (KM) mice and C57BL/6J mice were purchased from the Experimental Animal Center of Guangdong Province, China. KM mice were used to isolate primary Leydig cells for *in vitro* expriments and C57BL/6J mice were used for *in vivo* experiments. Animals were maintained under 12-h light/dart cycle at controlled temperature

Figure 5. m6A modification down-regulates the expression of miR-300-3p in LCs via the SMURF2/p-SMAD2 axis

(A) RNA m^{6}A modification levels in testes of chow-fed and HFD mice were determined by colorimetry. (B) The protein levels of METTL3, METTL14, and ALKBH5 in testes of HFD mice and chow-fed mice. (C and D) The mRNA levels of *Mettl3* and miR-300-3p in LCs overexpressing *Mettl3* for 48 h. (E and F) The mRNA levels of *Mettl3* and miR-300-3p in LCs with si-*Mettl3* for 48 h. (G) The protein levels of METTL3, p-SMAD2, SMAD2, SMAD3, and SMURF2 in LCs transfected with the *Mettl3* overexpressed vector for 48 h. (H) The protein levels of METTL3, p-SMAD2, SMAD2, SMAD3, and SMURF2 in LCs with si-*Mettl3* for 48 h. (I) Schematic of the positions of the m^{6}A motifs in *Smurf2* mRNA and (J) Schematic of mutated m^{6}A motifs (GGAC to GGCC) in the 3′-UTR of *Smurf2* gene. (K) Luciferase reporter vectors and a *Mettl3* overexpression vector were co-transfected into HEK293T cell for 48 h before the relative Renilla luciferase activity was measured and normalized to firefly luciferase activity. (L and M) The mRNA levels of *Smurf2* in LCs transfected for 24 h with *Mettl3* overexpression vector or *Mettl3* siRNA. (N) The potential binding site of SMAD2 in the miR-300 gene. (O) The expression of miR-300-3p in LCs after *Smad2* overexpression. (P) Schematic of the mutated 5′ upstream region of miR-300 in the PGL-3basic vector used to investigate the promoter motif of miR-300. (Q) Luciferase reporter vectors, the *Smad2* overexpression vector, and the PRL-TK vector were co-transfected into HEK293T cells for 48 h before the relative firefly luciferase activity was measured and normalized to the Renilla luciferase activity. (R) METTL3 regulates the expression of miR-300-3p via the SMURF2/p-SMAD2 axis. All data are presented as the mean ± SD from three independent experiments. $^{**}p < 0.01$, $^{***}p < 0.001$, $^{****}p < 0.0001$, and ns = not significant.

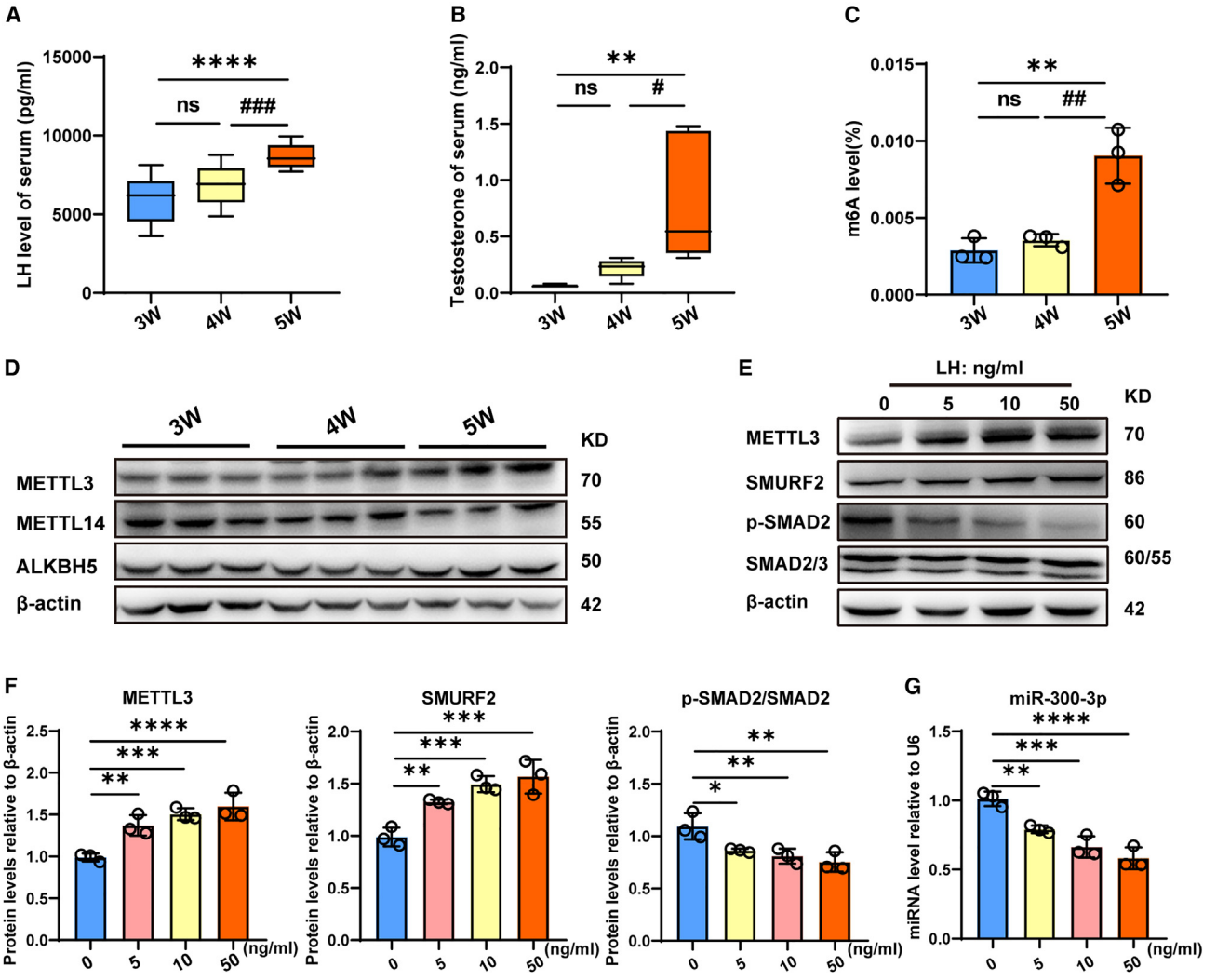

Figure 6. LH regulates METTL3 expression in LCs

(A) Serum LH concentration in mice at 3, 4, and 5 weeks of age. (B) Serum testosterone of mice at 3, 4, and 5 weeks of age was measured by RIA. (C) A colorimetric method was used to detect the m^6A modification level of LCs isolated respectively from 3-, 4-, and 5-week-old mice. (D) Western blotting showing the expression of METTL3, METTL14, and ALKBH5 in LCs isolated from 3-, 4-, and 5-week-old mice, respectively. (E) and (F) The protein levels of METTL3, SMURF2, p-SMAD2, and SAMD2 in LCs treated with different concentrations of LH for 24 h. (G) The expression of miR-300-3p in LCs treated with different LH concentrations for 24 h. All data are presented as the mean ± SD from three independent experiments. $^{**}p < 0.01$, $^{***}p < 0.001$, $^{****}p < 0.0001$, and ns = not significant.

(25 ± 1°C) and relative humidity of 50%–60%. Corresponding feed and drinking water were freely accessible. All animal experiments were conducted according to the National Institutes of Health guidelines for the care and use of animals and approved by the Institutional Animal Care and Use Committee of Jinan University (Approval No. 20200327-68).

Adult male volunteers recruited

Thirty adult men (aged 20–40 years) were recruited and divided into lean (BMI $\leq$24 kg/m^2, n = 11) and obesity (BMI $\geq$28 kg/m^2, n = 11) groups according to their BMI. Five milliliters of venous blood was collected from each person for serum testosterone detection and circulating RNA isolation. All experiments were performed in accordance with the Medical Ethics Committee of Sun Yat-Sen Memorial Hospital (Approval No.2021-YW-036).

HFD induced obesity model

Forty 4-week-old C57BL/6 mice were randomly divided into two groups, chow group and HFD group. All mice were fed with standard diet (26% kcal from fat) for 2 weeks to acclimatize before the experiment started. Then, mice of the chow group continued to be fed with standard diet while the mice of the HFD group were switched to an HFD (60% kcal from fat, D12492). The experiment was performed for 12 weeks, until the HFD mice were 20% heavier than the chow mice.

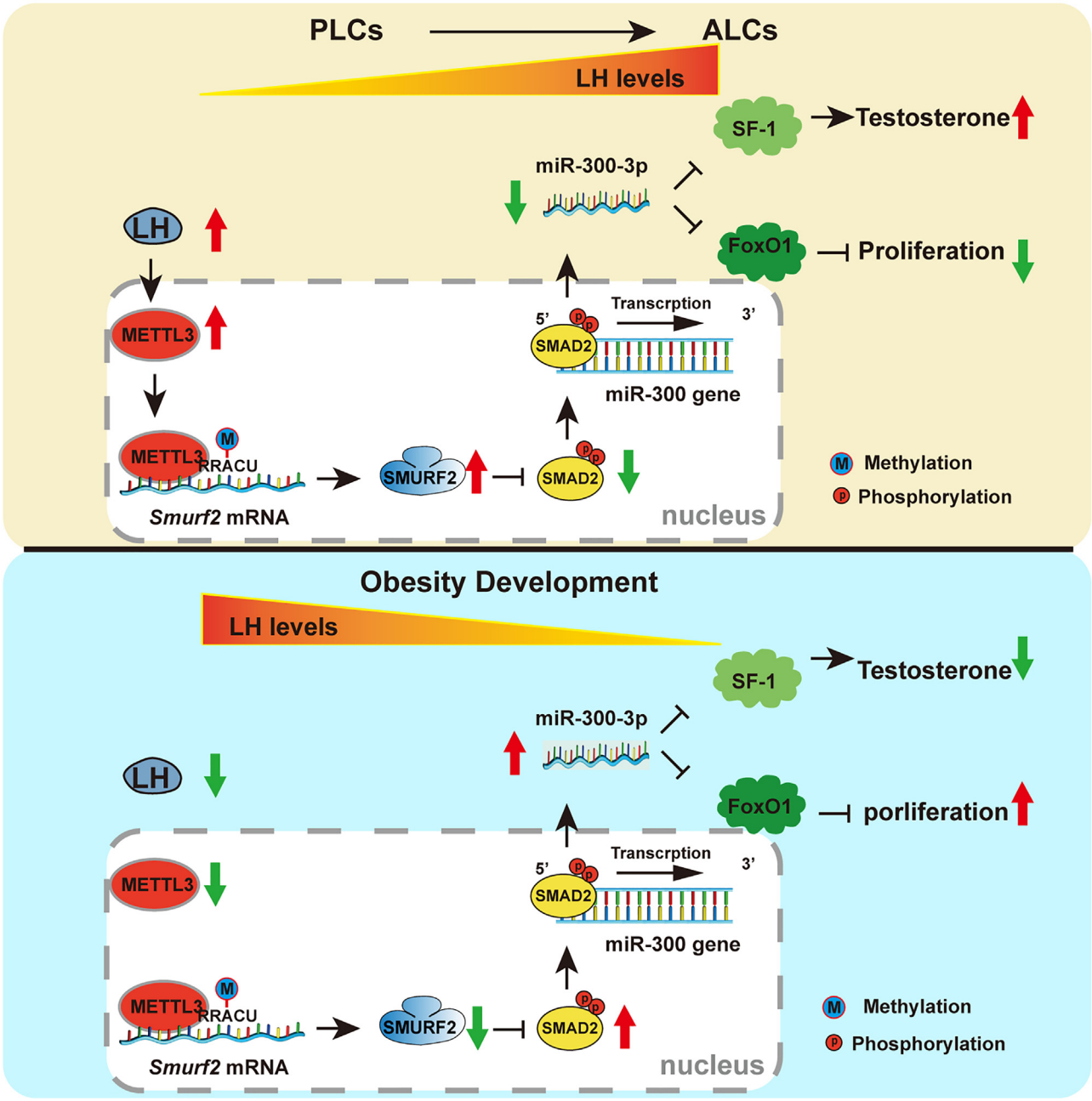

Figure 7. Schematic of the LH/METTL3/SMURF2/SMAD2/miR-300-3p axis that mediates testosterone synthesis in LCs

LH level progressively increased from PLC to ALC. In ALCs, LH induced METTL3 and SMURF2 expression by promoting METTL3 mediated m^{6}A modification of *Smurf2*, which suppressed miR-300-3p transcription by inhibiting p-SMAD2 levels. The reduction of miR-300-3p improved testosterone production and inhibited proliferation by upregulating SF-1 and FoxO1 expression in ALCs. The abnormally high expression of miR-300-3p observed in ALCs was involved in the regulation of obesity-related testosterone deficiency.

LCs isolation and culture

In rodents, fibroblast-like PLCs appear in the testis by postnatal day 14–21, while ALCs in testis are formed on postnatal days 49–56. Therefore, PLCs were isolated from 3-week-old male KM mice and ALCs were isolated from 8-week-old male KM mice.[57] Briefly, decapsulated testes were digested with collagenase type IV (Biosharp, China) at 1 mg/mL for 7 min at 37°C shaking water bath. The isolated cells were cultured in DMEM (Gibco, USA) with 10% FBS (ExCell Bio, China) for 1 h, and then the complete medium was changed to remove blood cells, spermatocytes, and Sertoli cells that adhered

slowly. Subsequently, the adherent cells were cultured in a cell incubator at 37°C in 5% CO_2. After 24 h, the cells were treated with hypotonic solution (20 mM Tris, pH 7.4) for 2 min to remove myoid cells. Cells were continually cultured for another 48 h to obtain LCs for subsequent experiments.

Western blot

The cells and testicular tissues were lysed in RIPA lysis buffer (Fude Bio, China) with 1 mM PMSF and protein phosphatase inhibitor (Roche, USA), and protein concentration was detected by BCA. Thirty micrograms of protein were electrophoresed on 12% SDS-PAGE and then transferred onto PVDF membranes. SF-1, CYP11A1, StAR, FoxO1, AKT, p-AKT, CCND1, CCND2, SMURF2, METTL3, METTL14, and ALKBH5 antibodies were added and incubated overnight at 4°C, and the blots were incubated with a secondary antibody labeled with horseradish peroxidase (HRP) for 1 h. Finally, the immunoreactions were detected by enhanced chemiluminescence (ECL) reagent. Antibody information is listed in Table S1.

Testosterone measurements

The concentration of testosterone in conditioned medium of LCs and serum testosterone concentration were measured with Iodine [^{125}I] Testosterone Radioimmunoassay Kit (Bejing North Institute of Biotechnology, China).

Serum miR-300-3p assay

RNA extraction

Total RNA was extracted from 300 μL serum samples using Trizol reagent (Life, USA). The collected RNA was dissolved in 20 μL RNase-free water, and used Nanodrop 2000 (Thermo Scientific, USA) to determine the quality. The purity range of the samples was 1.8–2.0 at wavelength 260/280, and the yield range was 400–1000 ng.

RT and quantitative real-time PCR

The RT and qRT-PCR were performed using 2 × All-in-One qPCR kit (Ribobio, China). DNA synthesized in 4 μL 5 × PAP/TR Buffer, 1 μL RTase Mix, 1 μL 2.5U/μL Ploy A Polymerase, and 400 ng RNA by performing incubation at 37°C for 60 min, and at 85°C for 5 min. Cel-miR-39-3p was used as external control to evaluate the relative expression of miR-300-3p. Two microliters of cDNA was used as template placed in 20 μL total reaction volume containing 10 μL 2 × All-in-One qPCR Mix, 2 μL adaptor primer, 2 μL miR-300-3p primer, and 4 μL nuclease-Free water. Then qRT-PCR was done using BioRad CFX manager system (BioRad, USA) at initial activation of 95°C for 10 min, followed by 40 cycles of 95°C for 10 s and 60°C for 20 s and 72°C for 10 s. The relative expression of miR-300-3p was calculated by the 2-$^{\Delta\Delta}$Ct method after normalization to cel-miR-39-3p.

Testicular injection of miR-300-3p agonist and antagonist

miR-300-3p agomir, antagomir, and their respective control (NC agomir and NC antagomir) were purchased from Ribobio (Guangzhou, China); 50 nmol of nucleic acid drugs were dissolved in 400 μL PBS. Each testis was injected with 15 μL of nucleic acid containing 1.875 nmol siRNA through the rete testes into the interstitial space using a microinjection pump (SPLab01, DK infusetek). A microinjector was inserted into one-third of the testis from outside the scrotum of mice, and the injection parameter was set to the flow rate of 15 μL/min. After injection, the needle was left for 30 s until the drug was fully absorbed. The sequence of miR-300-3p agomir and antagomir is listed in Table S2.

Histological analysis

The testis samples were fixed with 4% paraformaldehyde and embedded in paraffin wax following standard procedures. Sections of 5-μm thickness were prepared and stained with H&E for regular histological analysis. Briefly, dried sections were deparaffinized and stained with hematoxylin, then destained using 70% ethanol. Sections were then stained with eosin, destained, and dehydrated in ascending ethanol solutions. Sections were rinsed in xylene then cover-slipped with synthetic mounting media. Bright field images of the stains were obtained using using an ECLIPSE Ni-U upright microscope (Nikon).

For *in situ* hybridization (ISH) detection of miR-300-3p, the digoxigenin-labeled probe and *in situ* hybridization kit (MK1030) were purchased from Boster (Wuhan, China). In brief, the sections were dewaxed in xylene, rehydrated in gradient alcohol and distilled water, and endogenous enzymes were inactivated in 3% H_2O_2. mRNA in the tissue was exposed after pepsin digestion for 20 min. Prehybridization was conducted for 2–4 h at 42°C, followed by miR-300-3p probe hybridization overnight at 42°C. Then unhybridized probes were washed away with saline sodium citrate, and non-specific adhesion sites were blocked with 5% bovine serum albumin (BSA) for 30 min at 37°C. Tissues were then incubated with biotinylated anti-digoxin antibody for 60 min at 37°C, followed by incubation with streptavidin biotin-peroxidase complex (SABC) for 30 min at 37°C, and incubation with HRP for 20 min at 37°C. Finally, DAB was used for chromogenesis and hematoxylin for nuclear counterstaining. Images were captured using an ECLIPSE Ni-U upright microscope (Nikon) and analyzed by ImageJ software.

For immunofluorescence, frozen testis sections were fixed in acetone for 5 min and treated with 0.5% Triton X- for 10 min. Non-specific adhesion sites were blocked with 5% BSA at room temperature for 1 h. Primary and secondary antibodies were diluted in 5% BSA at 1:200. Tissues were incubated with primary antibodies overnight at 4°C, and then with secondary antibodies for 1 h at room temperature. Nuclei were stained with DAPI for 10 min. Fluorescence signals were captured and analyzed with an ECLIPSE Ni-U upright microscope (Nikon) and ImageJ software. Antibody details are listed in Table S1.

miR-300 promotor activity assay

MiR-300 promotor activity was measured by dual luciferase assay. Briefly, the potential transcription factors and promoter regions of miR-300 gene were predicted by JASPAR database. Then, the sequences containing miR-300 promoter sequences (−587/−4) were mutated, and the WT and mutation sequences were constructed into the PGL3-Basic vector respectively. HEK293T cells were

transfected with WT or mutation PGL3-Basic-300 vector, together with pcDNA3.1-Smad2 and PRL-TK. Transcriptional activity was determined by a luminometer, using a dual luciferase assay kit. Renilla luciferase (R-luc) was used to normalize firefly luciferase (F-luc) activity to evaluate reporter translation efficiency.

m^6A methylation modification detection by colorimetric method

Total RNA from LCs of mice at 3, 4, and 5 weeks of age were isolated by Trizol reagent. Then, m^6A modification levels were detected by m^6A RNA methylation quantification kit (Epigentek, USA) according to the manufacturer's instructions.

Luciferase reporter assay

Luciferase reporter assay was performed using the Dual Glo Luciferase Assay System Kit (Promega, USA) according to the manufacturer's instructions. Briefly, HEK-293T cells were co-transfected with luciferase reporter vectors (psi-check 2, psi-check 2-WT, psi-check 2-MU1, psi-check 2-MU2, psi-check 2-MU3. psi-check 2-MU4. psi-check 2-MU5, or psi-check 2-MU6) and pcDNA 3.1-*Mettl3* in a 96-well plate. After transfection for 48 h, cells were analyzed with the Dual Glo Luciferase Assay System Kit. F-luc was used to normalize R-luc activity to evaluate reporter translation efficiency.

Statistical analyses

All experiments were repeated at least three times, and data were expressed as the mean values ±SD. More than six sections from each testis were analyzed for morphological evaluation. Statistical analyses were performed with unpaired Student's t test or one-way ANOVA for more than two groups. GraphPad Prism 8 was used for data processing and plotting. P values less than 0.05 were considered significant and were marked as follows: $p < 0.05$ (*), $p < 0.01$ (**) and $p < 0.001$ (***).

DATA AVAILABILITY

The data that support the findings of this study are available from the corresponding author upon reasonable request.

SUPPLEMENTAL INFORMATION

Supplemental information can be found online at https://doi.org/10.1016/j.omtn.2023.03.016.

ACKNOWLEDGMENTS

This work was supported by National Natural Science Foundation of China (No. U22A20277, 32170865, and 82071634); Natural Science Foundation of Guangdong Province (No. 2022A1515012178, 2020A1515110963); Guangdong Clinical Research Center for Metabolic Diseases (2020B1111170009); The Science and Technology Plan Project of Guangzhou (No. 201508020001, 2016A020214013, 201803010044, 201704YG066, 2020A1515011203, 202102020261, 202103030003); Guangzhou Science and Technology Program Key Project (No. 201803010044).

AUTHOR CONTRIBUTIONS

J.L.L. and D.R.C. conceived this project; J.Y.X., S.Y.W., and Y.L. performed and analyzed the experiments; C.Z.W. provided clinical samples; Z.Y.W., Y.Q.F., Y.L.L., M.R.H., J.X.D., and Y.X.W. analyzed data and recorded the experiments; Q.H.Z. contributed analytic tools; Y.Y. and Y.D.H. designed the research and wrote the paper.

DECLARATION OF INTERESTS

The authors declare no competing interests.

REFERENCES

1. Wang, Y., Ni, C., Li, X., Lin, Z., Zhu, Q., Li, L., and Ge, R.S. (2019). Phthalate-induced fetal leydig cell dysfunction mediates male reproductive tract anomalies. Front. Pharmacol. *10*, 1309. https://doi.org/10.3389/fphar.2019.01309.
2. Zhou, R., Wu, J., Liu, B., Jiang, Y., Chen, W., Li, J., He, Q., and He, Z. (2019). The roles and mechanisms of Leydig cells and myoid cells in regulating spermatogenesis. Cell. Mol. Life Sci. *76*, 2681–2695. https://doi.org/10.1007/s00018-019-03101-9.
3. Ge, R.S., Dong, Q., Sottas, C.M., Papadopoulos, V., Zirkin, B.R., and Hardy, M.P. (2006). In search of rat stem Leydig cells: identification, isolation, and lineage-specific development. Proc. Natl. Acad. Sci. USA *103*, 2719–2724. https://doi.org/10.1073/pnas.0507692103.
4. Jarow, J.P., and Zirkin, B.R. (2005). The androgen microenvironment of the human testis and hormonal control of spermatogenesis. Ann. N. Y. Acad. Sci. *1061*, 208–220. https://doi.org/10.1196/annals.1336.023.
5. Chimento, A., Sirianni, R., Casaburi, I., and Pezzi, V. (2014). Role of estrogen receptors and g protein-coupled estrogen receptor in regulation of hypothalamus-pituitary-testis axis and spermatogenesis. Front. Endocrinol. *5*, 1. https://doi.org/10.3389/fendo.2014.00001.
6. Mendis-Handagama, S.M. (1997). Luteinizing hormone on Leydig cell structure and function. Histol. Histopathol. *12*, 869–882.
7. Sinha Hikim, A.P., and Swerdloff, R.S. (1999). Hormonal and genetic control of germ cell apoptosis in the testis. Rev. Reprod. *4*, 38–47. https://doi.org/10.1530/ror.0.0040038.
8. Williams-Ashman, H.G. (1983). Regulatory features of seminal vesicle development and function. Curr. Top. Cell. Regul. *22*, 201–275. https://doi.org/10.1016/b978-0-12-152822-5.50011-7.
9. Lei, Z.M., Mishra, S., Zou, W., Xu, B., Foltz, M., Li, X., and Rao, C.V. (2001). Targeted disruption of luteinizing hormone/human chorionic gonadotropin receptor gene. Mol. Endocrinol. *15*, 184–200. https://doi.org/10.1210/mend.15.1.0586.
10. Yang, M., Guan, S., Tao, J., Zhu, K., Lv, D., Wang, J., Li, G., Gao, Y., Wu, H., Liu, J., et al. (2021). Melatonin promotes male reproductive performance and increases testosterone synthesis in mammalian Leydig cells. Biol. Reprod. *104*, 1322–1336. https://doi.org/10.1093/biolre/ioab046.
11. Gregoraszczuk, E.Ł., and Rak-Mardyła, A. (2013). Supraphysiological leptin levels shift the profile of steroidogenesis in porcine ovarian follicles toward progesterone and testosterone secretion through increased expressions of CYP11A1 and 17b-HSD: a tissue culture approach. Reproduction *145*, 311–317. https://doi.org/10.1530/rep-12-0269.
12. Lardone, M.C., Argandoña, F., Lorca, M., Piottante, A., Flórez, M., Palma, C., Ebensperger, M., and Castro, A. (2018). Leydig cell dysfunction is associated with post-transcriptional deregulation of CYP17A1 in men with Sertoli cell-only syndrome. Mol. Hum. Reprod. *24*, 203–210. https://doi.org/10.1093/molehr/gay006.
13. Wu, X., Guo, X., Wang, H., Zhou, S., Li, L., Chen, X., Wang, G., Liu, J., Ge, H.S., and Ge, R.S. (2017). A brief exposure to cadmium impairs Leydig cell regeneration in the adult rat testis. Sci. Rep. *7*, 6337. https://doi.org/10.1038/s41598-017-06870-0.
14. Chen, H., Guo, X., Xiao, X., Ye, L., Huang, Y., Lu, C., and Su, Z. (2019). Identification and functional characterization of microRNAs in rat Leydig cells during development from the progenitor to the adult stage. Mol. Cell. Endocrinol. *493*, 110453. https://doi.org/10.1016/j.mce.2019.110453.
15. Liang, J., Li, H., Mei, J., Cao, Z., Tang, Y., Huang, R., Xia, H., Zhang, Q., Xiang, Q., Yang, Y., and Huang, Y. (2021). Sertoli cell-derived exosome-mediated transfer of

miR-145-5p inhibits Leydig cell steroidogenesis by targeting steroidogenic factor 1. Faseb. J. *35*, e21660. https://doi.org/10.1096/fj.202002589RRRR.

16. Duan, P., Huang, X., Ha, M., Li, L., and Liu, C. (2020). miR-142-5p/DAX1-dependent regulation of P450c17 contributes to triclosan-mediated testosterone suppression. Sci. Total Environ. *717*, 137280. https://doi.org/10.1016/j.scitotenv.2020.137280.

17. Gao, S., Li, C., Xu, Y., Chen, S., Zhao, Y., Chen, L., Jiang, Y., Liu, Z., Fan, R., Sun, L., et al. (2017). Differential expression of microRNAs in TM3 Leydig cells of mice treated with brain-derived neurotrophic factor. Cell Biochem. Funct. *35*, 364–371. https://doi.org/10.1002/cbf.3283.

18. An, S.Y., Zhang, G.M., Liu, Z.F., Zhou, C., Yang, P.C., and Wang, F. (2019). MiR-1197-3p regulates testosterone secretion in goat Leydig cells via targeting PPARGC1A. Gene *710*, 131–139. https://doi.org/10.1016/j.gene.2019.05.057.

19. Zhang, J., Zhang, J., Zhang, D., Ni, W., Xiao, H., and Zhao, B. (2020). Down-regulation of LINC00472 promotes osteosarcoma tumorigenesis by reducing FOXO1 expressions via miR-300. Cancer Cell Int. *20*, 100. https://doi.org/10.1186/s12935-020-01170-6.

20. Wang, L., and Yu, P. (2016). miR-300 promotes proliferation and EMT-mediated colorectal cancer migration and invasion by targeting p53. Oncol. Rep. *36*, 3225–3232. https://doi.org/10.3892/or.2016.5193.

21. Cruz, F.M., Tomé, M., Bernal, J.A., and Bernad, A. (2015). miR-300 mediates Bmi1 function and regulates differentiation in primitive cardiac progenitors. Cell Death Dis. *6*, e1953. https://doi.org/10.1038/cddis.2015.255.

22. Pan, P., Ma, F., Wu, K., Yu, Y., Li, Y., Li, Z., Chen, X., Huang, T., Wang, Y., and Ge, R-s (2020). Maternal exposure to zearalenone in masculinization window affects the fetal Leydig cell development in rat male fetus. Environ. Pollut. *263*, 114357. https://doi.org/10.1016/j.envpol.2020.114357.

23. Kang, Y., Zhang, Y., Sun, Y., Wen, Y., and Sun, F. (2018). MicroRNA-300 suppresses metastasis of oral squamous cell carcinoma by inhibiting epithelial-to-mesenchymal transition. OncoTargets Ther. *11*, 5657–5666. https://doi.org/10.2147/ott.S173236.

24. Honda, S., Morohashi, K., Nomura, M., Takeya, H., Kitajima, M., and Omura, T. (1993). Ad4BP regulating steroidogenic P-450 gene is a member of steroid hormone receptor superfamily. J. Biol. Chem. *268*, 7494–7502.

25. Lynch, J.P., Lala, D.S., Peluso, J.J., Luo, W., Parker, K.L., and White, B.A. (1993). Steroidogenic factor 1, an orphan nuclear receptor, regulates the expression of the rat aromatase gene in gonadal tissues. Mol. Endocrinol. *7*, 776–786. https://doi.org/10.1210/mend.7.6.8395654.

26. Lala, D.S., Rice, D.A., and Parker, K.L. (1992). Steroidogenic factor I, a key regulator of steroidogenic enzyme expression, is the mouse homolog of fushi tarazu-factor I. Mol. Endocrinol. *6*, 1249–1258. https://doi.org/10.1210/mend.6.8.1406703.

27. Val, P., Lefrançois-Martinez, A.M., Veyssière, G., and Martinez, A. (2003). SF-1 a key player in the development and differentiation of steroidogenic tissues. Nucl. Recept. *1*, 8. https://doi.org/10.1186/1478-1336-1-8.

28. Aoki, M., Jiang, H., and Vogt, P.K. (2004). Proteasomal degradation of the FoxO1 transcriptional regulator in cells transformed by the P3k and Akt oncoproteins. Proc. Natl. Acad. Sci. USA *101*, 13613–13617.

29. Zhao, B.S., Roundtree, I.A., and He, C. (2017). Post-transcriptional gene regulation by mRNA modifications. Nat. Rev. Mol. Cell Biol. *18*, 31–42. https://doi.org/10.1038/nrm.2016.132.

30. Kierzek, E., and Kierzek, R. (2003). The thermodynamic stability of RNA duplexes and hairpins containing N6-alkyladenosines and 2-methylthio-N6-alkyladenosines. Nucleic Acids Res. *31*, 4472–4480. https://doi.org/10.1093/nar/gkg633.

31. Li, Y., Zhang, Q., Cui, G., Zhao, F., Tian, X., Sun, B.F., Yang, Y., and Li, W. (2020). m(6)A regulates liver metabolic disorders and hepatogenous diabetes. Dev. Reprod. Biol. *18*, 371–383. https://doi.org/10.1016/j.gpb.2020.06.003.

32. Li, X., Wang, Z., Jiang, Z., Guo, J., Zhang, Y., Li, C., Chung, J., Folmer, J., Liu, J., Lian, Q., et al. (2016). Regulation of seminiferous tubule-associated stem Leydig cells in adult rat testes. Proc. Natl. Acad. Sci. USA *113*, 2666–2671. https://doi.org/10.1073/pnas.1519395113.

33. Miller, W.L., and Auchus, R.J. (2011). The molecular biology, biochemistry, and physiology of human steroidogenesis and its disorders. Endocr. Rev. *32*, 81–151. https://doi.org/10.1210/er.2010-0013.

34. Martin, L.J. (2016). Cell interactions and genetic regulation that contribute to testicular Leydig cell development and differentiation. Mol. Reprod. Dev. *83*, 470–487. https://doi.org/10.1002/mrd.22648.

35. Zirkin, B.R., and Ewing, L.L. (1987). Leydig cell differentiation during maturation of the rat testis: a stereological study of cell number and ultrastructure. Anat. Rec. *219*, 157–163. https://doi.org/10.1002/ar.1092190208.

36. Zirkin, B.R., and Papadopoulos, V. (2018). Leydig cells: formation, function, and regulation. Biol. Reprod. *99*, 101–111. https://doi.org/10.1093/biolre/ioy059.

37. Morohashi, K.I., and Omura, T. (1996). Ad4BP/SF-1, a transcription factor essential for the transcription of steroidogenic cytochrome P450 genes and for the establishment of the reproductive function. Faseb. J. *10*, 1569–1577. https://doi.org/10.1096/fasebj.10.14.9002548.

38. Yazawa, T., Mizutani, T., Yamada, K., Kawata, H., Sekiguchi, T., Yoshino, M., Kajitani, T., Shou, Z., Umezawa, A., and Miyamoto, K. (2006). Differentiation of adult stem cells derived from bone marrow stroma into Leydig or adrenocortical cells. Endocrinology *147*, 4104–4111. https://doi.org/10.1210/en.2006-0162.

39. Yazawa, T., Inanoka, Y., Mizutani, T., Kuribayashi, M., Umezawa, A., and Miyamoto, K. (2009). Liver receptor homolog-1 regulates the transcription of steroidogenic enzymes and induces the differentiation of mesenchymal stem cells into steroidogenic cells. Endocrinology *150*, 3885–3893. https://doi.org/10.1210/en.2008-1310.

40. Gondo, S., Okabe, T., Tanaka, T., Morinaga, H., Nomura, M., Takayanagi, R., Nawata, H., and Yanase, T. (2008). Adipose tissue-derived and bone marrow-derived mesenchymal cells develop into different lineage of steroidogenic cells by forced expression of steroidogenic factor 1. Endocrinology *149*, 4717–4725. https://doi.org/10.1210/en.2007-1808.

41. Yang, Y., Su, Z., Xu, W., Luo, J., Liang, R., Xiang, Q., Zhang, Q., Ge, R.S., and Huang, Y. (2015). Directed mouse embryonic stem cells into leydig-like cells rescue testosterone-deficient male rats in vivo. Stem Cells Dev. *24*, 459–470. https://doi.org/10.1089/scd.2014.0370.

42. Glass, A.R., Swerdloff, R.S., Bray, G.A., Dahms, W.T., and Atkinson, R.L. (1977). Low serum testosterone and sex-hormone-binding-globulin in massively obese men. J. Clin. Endocrinol. Metab. *45*, 1211–1219. https://doi.org/10.1210/jcem-45-6-1211.

43. Allan, C.A., and McLachlan, R.I. (2010). Androgens and obesity. Curr. Opin. Endocrinol. Diabetes Obes. *17*, 224–232. https://doi.org/10.1097/MED.0b013e3283398ee2.

44. Van de Velde, F., Reyns, T., Toye, K., Fiers, T., Kaufman, J.M., T'Sjoen, G., and Lapauw, B. (2020). The effects of age and obesity on postprandial dynamics of serum testosterone levels in men. Clin. Endocrinol. *92*, 214–221. https://doi.org/10.1111/cen.14141.

45. Hausser, J., Syed, A.P., Bilen, B., and Zavolan, M. (2013). Analysis of CDS-located miRNA target sites suggests that they can effectively inhibit translation. Genome Res. *23*, 604–615. https://doi.org/10.1101/gr.139758.112.

46. Liu, G., Zhang, R., Xu, J., Wu, C.I., and Lu, X. (2015). Functional conservation of both CDS- and 3'-UTR-located microRNA binding sites between species. Mol. Biol. Evol. *32*, 623–628. https://doi.org/10.1093/molbev/msu323.

47. Rigoutsos, I. (2009). New tricks for animal microRNAS: targeting of amino acid coding regions at conserved and nonconserved sites. Cancer Res. *69*, 3245–3248. https://doi.org/10.1158/0008-5472.CAN-09-0352.

48. Accili, D., and Arden, K.C. (2004). FoxOs at the crossroads of cellular metabolism, differentiation, and transformation. Cell *117*, 421–426.

49. Vivar, R., Humeres, C., Muñoz, C., Boza, P., Bolivar, S., Tapia, F., Lavandero, S., Chiong, M., and Diaz-Araya, G. (2016). FoxO1 mediates TGF-beta1-dependent cardiac myofibroblast differentiation. Biochim. Biophys. Acta *1863*, 128–138. https://doi.org/10.1016/j.bbamcr.2015.10.019.

50. Sinha, D., Kalimutho, M., Bowles, J., Chan, A.L., Merriner, D.J., Bain, A.L., Simmons, J.L., Freire, R., Lopez, J.A., Hobbs, R.M., et al. (2018). Cep55 overexpression causes male-specific sterility in mice by suppressing Foxo1 nuclear retention through sustained activation of PI3K/Akt signaling. FASEB J *32*, 4984–4999. https://doi.org/10.1096/fj.201701096RR.

51. Alarcón, C.R., Lee, H., Goodarzi, H., Halberg, N., and Tavazoie, S.F. (2015). N6-methyladenosine marks primary microRNAs for processing. Nature *519*, 482–485. https://doi.org/10.1038/nature14281.

52. Wang, Y., Gao, M., Zhu, F., Li, X., Yang, Y., Yan, Q., Jia, L., Xie, L., and Chen, Z. (2020). METTL3 is essential for postnatal development of brown adipose tissue and energy expenditure in mice. Nat. Commun. *11*, 1648. https://doi.org/10.1038/s41467-020-15488-2.

53. Xie, W., Ma, L.L., Xu, Y.Q., Wang, B.H., and Li, S.M. (2019). METTL3 inhibits hepatic insulin sensitivity via N6-methyladenosine modification of Fasn mRNA and promoting fatty acid metabolism. Biochem. Biophys. Res. Commun. *518*, 120–126. https://doi.org/10.1016/j.bbrc.2019.08.018.

54. Chen, Y., Wang, J., Xu, D., Xiang, Z., Ding, J., Yang, X., Li, D., and Han, X. (2021). m(6)A mRNA methylation regulates testosterone synthesis through modulating autophagy in Leydig cells. Autophagy *17*, 457–475. https://doi.org/10.1080/15548627.2020.1720431.

55. Liu, K., Ding, Y., Ye, W., Liu, Y., Yang, J., Liu, J., and Qi, C. (2016). Structural and functional characterization of the proteins responsible for N(6)-methyladenosine modification and recognition. Curr. Protein Pept. Sci. *17*, 306–318.

56. Lin, X., Liang, M., and Feng, X.H. (2000). Smurf2 is a ubiquitin E3 ligase mediating proteasome-dependent degradation of Smad2 in transforming growth factor-beta signaling. J. Biol. Chem. *275*, 36818–36822. https://doi.org/10.1074/jbc.C000580200.

57. Liang, J., Tang, Y., Li, H., Mei, J., Cao, Z., Xia, H., Huang, R., Yang, Y., and Huang, Y. (2021). Isolation of primary leydig cells from murine testis. Bio. Protoc. *11*, e4223. https://doi.org/10.21769/BioProtoc.4223.